https://doi.org/10.5194/amt-2020-13
Preprint. Discussion started: 3 February 2020

Atmospheric Measurement Techniques Discussions

A Vacuum Ultraviolet Ion Source (VUV-IS) for Iodide-Chemical Ionization Mass Spectrometry: A Substitute for Radioactive Ion Sources

Yi Ji[1], L. Gregory Huey[1], David J. Tanner[1], Young Ro Lee[1], Patrick R. Veres[2], J. Andrew Neuman[2,3], Yuhang Wang[1], Xinming Wang[4]

[1]School of Earth and Atmospheric Sciences, Georgia Institute of Technology, Atlanta, GA 30332, USA
[2]NOAA Earth System Research Laboratory (ESRL) Chemical Science Division, Boulder, Colorado, USA, 80305
[3]Cooperative Institute for Research in Environmental Sciences, University of Colorado Boulder, Boulder, Colorado, USA, 80309
[4]State Key Laboratory of Organic Geochemistry, Guangzhou Institute of Geochemistry, Chinese Academy of Sciences, Guangzhou 510640, China

Correspondence to: L. Gregory Huey (greg.huey@eas.gatech.edu)

Abstract. A new ion source (IS) utilizing vacuum ultraviolet (VUV) light is developed and characterized for use with iodide-chemical ionization mass spectrometers (I^--CIMS). The VUV-IS utilizes a compact krypton lamp that emits light in two wavelength bands corresponding to energies of ~10.0 and 10.6 eV. The VUV light photoionizes either methyl iodide (ionization potential, IP = 9.54 ± 0.02 eV) or benzene (IP = 9.24378 ± 0.00007 eV) to form cations and photoelectrons. The electrons react with methyl iodide to form I^- which serves as the reagent ion for the CIMS. The VUV-IS is characterized by measuring the sensitivity of a quadrupole CIMS (Q-CIMS) to formic acid, molecular chlorine, and nitryl chloride under a variety of flow and pressure conditions. The sensitivity of the Q-CIMS, with the VUV-IS, reached up to ~700 Hz $pptv^{-1}$, with detection limits of less than 1 pptv for a one minute integration period. The reliability of the Q-CIMS with a VUV-IS is demonstrated with data from a month long ground-based field campaign. The VUV-IS is further tested by operation on a high resolution time-of-flight CIMS (TOF-CIMS). Sensitivities greater than 25 Hz $pptv^{-1}$ were obtained for formic acid and molecular chlorine, which were similar to that obtained with a radioactive source. In addition, the mass spectra from sampling ambient air was cleaner with the VUV-IS on the TOF-CIMS compared to measurements using a radioactive source. These results demonstrate that the VUV lamp is a viable substitute for radioactive ion sources on I^--CIMS systems for most applications. In addition, the VUV-IS can likely be extended to other reagent ions, such as SF_6^- which are formed from high IP electron attachers, by the use of absorbers such as benzene to serve as a source of photoelectrons.

https://doi.org/10.5194/amt-2020-13
Preprint. Discussion started: 3 February 2020

Atmospheric Measurement Techniques Discussions

1 Introduction

Chemical ionization mass spectrometry (CIMS) has been widely used as a powerful tool to measure various atmospheric compounds with high sensitivity and fast time response. CIMS measurements are based on selective ionization of compounds in air by reagent ions via ion molecule reactions. CIMS using the iodide anion (I^-) and its water clusters as reagent ions (I^--CIMS) has been widely used in the measurements of many atmospheric trace gases, e.g. bromine oxide (BrO) and peroxyacyl nitric anhydride (PAN) (Slusher et al., 2004;Huey, 2007;Phillips et al., 2013;Lee et al., 2014;Liao et al., 2014;Neuman et al., 2016;Liu et al., 2017;Priestley et al., 2018;Bertram et al., 2011;Thornton et al., 2010;Osthoff et al., 2008).

Typically, I^--CIMS systems use a radioactive isotope, usually ^{210}Po, as an ion source. ^{210}Po emits α particles (with an energy of ~5 MeV) that directly ionize the carrier gas in the ion source to produce secondary electrons. The secondary electrons are thermalized by collisions and react with methyl iodide (CH_3I) to form I^- by dissociative electron attachment. The use of radioactive ion sources with the I^--CIMS system is well-established and has several important advantages. For example, radioactive sources are exceedingly reliable and are easy to use, as they require no external power. Radioactive sources often produce relatively clean mass spectra with little interfering masses. However, radioactive sources have several disadvantages as well. ^{210}Po is toxic and is highly regulated which often makes it difficult to transport, store, and use in remote locations. We have recently developed a lower activity ^{210}Po ion source that is subject to fewer regulatory restrictions (Lee et al., 2019). However, there remain applications where the use of any radioactivity is very difficult or prohibited. A more subtle disadvantage is that radioactive ion sources emit continuously, which can lead to the build up of interfering species. For these reasons, it is desirable to find a non-radioactive alternative to efficiently generate I^- and other reagent ions. Electrical discharges and x-ray ion sources have been used as ion sources in atmospheric pressure chemical ionization mass spectrometers (AP-CIMS) (Jost et al., 2003;Skalny et al., 2007;Kurten et al., 2011;Wang et al., 2017). However, they have not been commonly employed with I^--CIMS systems perhaps due to limited sensitivity and the generation of interfering ions. Recently Eger et al. (2019) developed a promising ion source using a radio frequency (RF) discharge on an I^--CIMS system, providing another alternative to radioactive sources albeit with lower signal levels. However, the RF source also generated high levels of other ions such as dicyanoiodate anion $I(CN)_2^-$, providing additional pathways for detecting species such as SO_2 and HCl.

In this work, we investigate the use of a small krypton (Kr) lamp as a substitute for a radioactive ion source on an I^--CIMS. Similar lamps have been commonly used in atmospheric pressure photoionization-mass spectrometry (Kauppila et al., 2017). The vacuum ultraviolet (VUV) light is generated from two emission lines centered at 117 (photon energy = 10.6 eV) and 124 nm (photon energy = 10 eV). CH_3I has a large absorption cross section (7×10^{-17} cm^2 $molecule^{-1}$) at these wavelengths and a relatively low ionization potential (IP =9.54 ± 0.02 eV) (Holmes and Lossing, 1991;Olney et al., 1998). Absorption of the VUV light by CH_3I forms cations and relatively low energy photoelectrons which can then be attached by CH_3I to form I^-. Benzene (C_6H_6) can also serve as a VUV absorber to produce photoelectrons as it has a larger absorption cross section and an

https://doi.org/10.5194/amt-2020-13
Preprint. Discussion started: 3 February 2020


Atmospheric Measurement Techniques Discussions

even lower IP (Nemeth et al., 1993;Capalbo et al., 2016). We explore the use of C_6H_6 as a source of photoelectrons as we have found that delivering even modest quantities of gas phase CH_3I to our ion source can be problematic as it has a tendency to polymerize to non-volatile species in compressed gas cylinders. Tests of C_6H_6 as a photoelectron source in this work are performed as it may enhance ion production when used in combination with lower levels of CH_3I. C_6H_6 may also be used as an electron source for use with other electron attaching compounds with higher IPs, such as SF_6, to form reagent ions such as SF_6^-.

The performance of the VUV-IS was characterized by measuring the sensitivities on a quadrupole CIMS (Q-CIMS) to formic acid, chlorine (Cl_2), and nitryl chloride ($ClNO_2$), under different flow conditions with varying levels of CH_3I. Similar tests were also performed using a flow of both C_6H_6 and CH_3I through the ion source. Potential interferences due to the VUV light interacting with air or surfaces are investigated by comparing ambient mass spectra obtained with a VUV-IS and a standard 20 mCi ^{210}Po ion source (NRD Static Control, P-2031) on both a commercial high resolution time-of-flight CIMS (TOF-CIMS) and a Q-CIMS. The reliability of the VUV-IS is tested by performing field measurements for a six week time period at a remote location.

2 Materials and Methods

2.1 Quadrupole I^--CIMS and experimental configurations

The Q-CIMS used here is very similar to the system that has measured a variety of species such as Cl_2, BrO, and PAN, and has been detailed in previous publications (Slusher et al., 2004;Liao et al., 2011;Liao et al., 2014;Lee et al., 2019). Details specific to these experiments are described below. A diagram of the I^--CIMS system and the experimental layout is shown in Figure 1. Varying levels of calibration standard were added to 4-10 standard liters per minute (slpm) of N_2 and delivered to the sampling inlet of the CIMS through perfluoroalkoxy (PFA) Teflon tubing, with dimensions of 1.27 cm outer diameter, and 0.95 cm inner diameter. Approximately 1.6 slpm of this flow was sampled into the CIMS flow tube and the rest was exhausted into the lab. The flow tube was humidified by adding 20 standard cubic centimeters per minute (sccm) of N_2 through a water bubbler kept in an ice bath. The flow tube was operated at a pressure of either 20 or 40 Torr by using either a 0.91 mm or 0.635 mm orifice between the flow tube and the collisional dissociation chamber (CDC). The scroll pump flow was controlled to maintain the flow tube at 20 or 40 Torr.

Mass spectra of ambient Atlanta air were obtained, in order to check for potential interferences due to the VUV-IS. For these experiments air was sampled from the roof of the Environmental Science and Technology building on the Georgia Tech campus. A PFA Teflon tube of 0.95 cm inner diameter and 8 m long was used as a sampling inlet. A total flow of ~7 slpm of ambient air was drawn through the inlet, of which 1.7 slpm was sampled into the CIMS flow tube and the rest was exhausted through a diaphragm pump. The flow tube was operated at 20 Torr.

https://doi.org/10.5194/amt-2020-13
Preprint. Discussion started: 3 February 2020


Atmospheric Measurement Techniques Discussions

95 **2.2 Calibration sources**

Permeation tubes (KIN-TEK Laboratories, Inc.) were used as the sources of Cl_2 and formic acid for tests on the Q-CIMS. The output of both tubes was measured by ion chromatography as detailed by Liao et al. (2011) and Nah et al. (2018). The permeation rates were measured to be 104.7 ng min^{-1} for formic acid and 14.8 ng min^{-1} for Cl_2. $ClNO_2$ standard gas was generated by passing a humidified flow of Cl_2 from the permeation tube in N_2 through a bed of sodium nitrite ($NaNO_2$). The
100 yield of $ClNO_2$ from Cl_2 was assumed to be 50% as we have consistently found in previous studies (Liu et al., 2017).

Sensitivity tests to formic acid and Cl_2 on a TOF-CIMS were performed by standard addition in laboratory air. The calibration species were obtained from a calibrated formic acid permeation device (47 ng min^{-1}) and a 4 ppm Cl_2 in N_2 compressed gas cylinder. The Cl_2 cylinder was calibrated by cavity ring-down spectroscopy (CRDS) at 405 nm. The permeation rate of formic
105 acid was measured by catalytic conversion to CO_2 followed by CO_2 detection as detailed by Veres et al (2010).

2.3 VUV ion source (VUV-IS)

In a typical I^--CIMS system, a flow of CH_3I in N_2 is passed through a ^{210}Po radioactive ion source, to form the reagent ion I^-.
110 In this study, the radioactive source was removed and replaced with a VUV lamp assembly. The Kr lamp is powered by a 4 W DC power supply. Two configurations (a and b as shown in Figure 1) of the VUV lamp assembly were tested. In both configurations a small Kr VUV lamp (Heraeus, Type No. PKS 106) (19.6 mm diameter × 53.5 mm length) was used to generate ions. This lamp is commonly used in small commercial VOC detectors that utilize photoionization as a detection method. The VUV lamp was operated at ~280 Volts DC and typically drew ~0.7 mA. In general, the ion current reaching the mass
115 spectrometer increased with increasing lamp voltage (see Figure S1). The VUV lamp was attached to a custom QF 40 centering ring with vacuum epoxy. The centering ring has a thru hole (11.4 mm diameter) with a counterbore (41.1 mm diameter) in the center. The lamp is sealed to the edge of the counterbore with vacuum epoxy. The thru hole allows light from the lamp to enter the ion source region of the CIMS. The QF 40 centering ring is mated on the low pressure side to an inline tee with two QF 40 flanges on the ends and a 0.635 cm NPT fitting in the center. In lamp configuration (a), the inline tee is attached to a
120 standard short QF 40 nipple (126 mm length) which serves as a photoionization region and provides a direct path for the VUV photons and generated ions into the flow tube. In configuration (b), a QF 40 90 degree elbow was attached between the QF 40 nipple and CIMS flow tube to prevent direct exposure of the flow tube to the VUV photons. The ambient pressure side of the QF 40 centering ring, on which the VUV lamp attached, is mated to a QF 40 × QF 16 × QF 40 reducing tee housing for protection of the VUV lamp. The QF 16 branch of the tee enables visual inspection of the lamp operation.
125

https://doi.org/10.5194/amt-2020-13
Preprint. Discussion started: 3 February 2020


Atmospheric Measurement Techniques Discussions

The sensitivity of the VUV-IS for measuring formic acid, Cl_2 and $ClNO_2$ was measured for varying CH_3I concentrations and at two flow tube pressures (Table 1 and 2). The impact of adding C_6H_6 was investigated by varying the concentration of C_6H_6 at a lower level of CH_3I. Compressed gas cylinders of ~700 ppmv of CH_3I and ~0.1% of C_6H_6 were used as CH_3I and C_6H_6 sources. A variable flow of N_2 containing CH_3I was delivered in the ion source to determine the optimal flow (Figure 2).

2.4 TOF-CIMS

The VUV-IS was also characterized by operation on a commercial TOF-CIMS (Aerodyne Research Incorporated) (Lee et al., 2014). The ion molecule reactor (IMR) used here was constructed from a 150 mm long QF 40 adapter tee with a 9.5 mm fitting in the center, to allow mounting of the VUV-IS. The VUV lamp mounted to the QF 40 inline tee (section 2.1) was attached to a QF 40 × QF 16 conical adapter connected to a flange with a 9.5 mm stainless steel tube. This allowed the VUV-IS assembly to be mated directly to the IMR using standard vacuum components. The IMR was maintained at a pressure of 30 torr and operated at a total flow of 2.2 slpm. A 1 slpm N_2 flow with 30-400 ppmv CH_3I passed through the VUV-IS into the IMR and mixed with 1.2 slpm of ambient air. Water was dynamically added to the IMR to maintain a constant ratio of I^- to $I^-(H_2O)$. This provided real-time compensation for changes in ambient humidity to minimize fluctuations in sensitivity. Mass spectra were obtained with both a VUV-IS and a standard radioactive ion source, sampling ambient air in Boulder Colorado.

3 Results

The sensitivity of the VUV-IS on the Q-CIMS can reach 100s of Hz $pptv^{-1}$ (Table 1 and 2) similar to the best sensitivity obtained with radioactive sources (e.g. Lee et al., 2019). Configuration (a) of the VUV-IS gives the highest signal levels (Figure 3) especially at lower flow rates through the ion source. However, configuration (a) also leads to significantly higher levels of interfering masses than configuration (b) due to photoelectrons being generated on the illuminated surface of the flow tube (Figure 4). Configuration (b) yields lower signals but significantly reduces background ion generation relative to configuration (a). The VUV-IS requires significantly higher levels of CH_3I than those used in radioactive sources (typically ~1 ppmv, Slusher et al., 2004) (Figure 3 and 5), because the CH_3I must also serve as a source of photoelectrons. C_6H_6 can be used as a VUV absorber to generate photoelectrons (Figure 3 and 5) without generating excessive interferences (Figure 4). Tests on the TOF-CIMS demonstrated that the VUV-IS and a standard radioactive ion source produced the same reagent ion (I^-) abundance. In addition, both sources generated similar mass spectra of ambient air, demonstrating that the VUV-IS source did not produce significant interferences to the detection of most trace gases (Figure 6).

3.1 Q-CIMS Sensitivities using CH_3I

The sensitivities and LODs for formic acid, Cl_2 and $ClNO_2$ under different experimental conditions using lamp configuration (b) are compiled in Table 1. With the flow tube at 20 Torr, sensitivities to formic acid, Cl_2 and $ClNO_2$ reached up to 147, 161

https://doi.org/10.5194/amt-2020-13
Preprint. Discussion started: 3 February 2020


Atmospheric Measurement Techniques Discussions

and 154 Hz pptv^{-1}, respectively, using up to 86.5 ppmv of CH_3I in the ion source flow. At 40 Torr, similar sensitivities (128, 149 and 148 Hz pptv^{-1} for formic acid, Cl_2 and $ClNO_2$, respectively) were achieved with less CH_3I (19.0 ppmv). Figure 5 shows the dependence of the CIMS sensitivities on CH_3I level at 20 Torr (upper left) and 40 Torr (lower left) with no other absorber added. In general, CIMS sensitivities increase with the CH_3I mixing ratio. However, the response is less than linear and appears to saturate at higher levels of absorber. With the maximum concentration of CH_3I (86.5 ppmv, 5.70×10^{13} molecule cm^{-3}) used in this experiment, ~8% of photons emitted from the VUV lamp were absorbed (see SI for sample calculation). This indicates that other factors such as ion recombination and wall loss could be limiting the ion abundance. The sensitivities and LODs under similar experimental conditions using lamp configuration (a) are show in Table 2 and Figure 3. The sensitivities to formic acid, Cl_2, and $ClNO_2$ approached ~700 Hz pptv^{-1}, with limits of dectection of less than 1 pptv for a one minute integration period. Limits of detection are defined at a signal-to-noise ratio of 3 where the noise is the variance of the background measurements. In general, the sensitivities using lamp configuration (a) were about a factor of four larger than in configuration (b). Note that all the Q-CIMS sensitivities reported in this work are not normalized to the reagent ion signal, since the reagent ion signal is not known accurately. We estimate the reagent ion signals are ~100 MHz at the highest sensitivities, but the Q-CIMS detector counts ions linearly only up to about 0.5 MHz.

3.2 Q-CIMS Sensitivities using CH_3I and C_6H_6

In order to test the effectiveness of the addition of another absorber to generate photoelectrons, mixtures of CH_3I and C_6H_6 were added to the ion source. Lower mixing ratios (8.8 ppmv at 20 Torr, 1.8 ppmv at 40 Torr) of CH_3I were used in combination with varying amounts of C_6H_6 to assess the impact of the addition of C_6H_6 to the generated ion current using lamp configuration (b). The sensitivity dependence on C_6H_6 mixing ratio is shown in Figure 5. At 20 Torr, up to 229.2 ppmv C_6H_6 was added to 8.8 ppmv CH_3I to achieve the equivalent sensitivity (158, 157, and 152 Hz pptv^{-1} for formic acid, Cl_2 and $ClNO_2$, respectively) using 86.5 ppmv CH_3I alone. At 40 Torr, up to 58.9 ppmv C_6H_6 was added to 1.8 ppmv of CH_3I to reach the maximum level of sensitivities (157, 166, and 138 Hz pptv^{-1} for formic acid, Cl_2 and $ClNO_2$, respectively) when using 19.0 ppmv of CH_3I. Similar trends for the addition of C_6H_6 using lamp configuration (a) was observed and are shown in Table 2 and Figure 3. At both 20 and 40 Torr sensitivities of more than 600 Hz pptv^{-1} were obtained for all species in configuration (a). These results demonstrate that addition of an absorber (e.g. benzene) enables high sensitivity with the VUV-IS while adding typical levels (a few ppmv) of an electron attaching compound.

3.3 Q-CIMS Interference Tests

Representative mass spectra (m/z = 20 - 220 amu) taken with a 20 mCi ^{210}Po standard radioactive source and the VUV-IS with configuration (a) on an I$^-$-CIMS sampling ambient air are shown in Figure 4. Note that the I$^-$ signal is saturated in all mass spectra due to the very high signal levels. Clearly, the VUV-IS in configuration (a) generates many additional ions compared to a radioactive source. Large signals (> 100,000 Hz) are observed at O_2^- (m/z = 32 amu), NO_3^- (m/z = 62 amu), and CO_3^- (m/z

https://doi.org/10.5194/amt-2020-13
Preprint. Discussion started: 3 February 2020


Atmospheric Measurement Techniques Discussions

= 60 amu). This indicates that photoelectrons generated on the illuminated surface of the flow tube in the presence of the sampled air leads to formation of O_2^- by electron attachment to O_2. This also leads to the formation of CO_3^- and NO_3^- by subsequent reactions with CO_2, O_3, and NO_2 (Mohler and Arnold, 1991). Consequently, the generation of O_2^- initiates significant secondary chemistry that may lead to interfering signals at a large number of masses.

Using the VUV-IS in configuration (b) prevents direct illumination of the flow tube by the VUV lamp and produces similar spectra to those obtained with a radioactive source (Figure 4). The O_2^- signal levels are lower by more than three orders of magnitude compared to configuration (a) where the flow tube is directly illuminated.

Finally, Figure 4 also has a mass spectrum using the VUV-IS in configuration (b) with the addition of 110 ppmv of C_6H_6 and 8.8 ppmv of CH_3I in the ion source flow. The addition of the C_6H_6 does not produce significant amounts of additional ions and the mass spectra is very similar to that obtained without C_6H_6. This indicates that using C_6H_6 (or other low IP compounds) as a light absorber to generate photoelectrons has the potential to extend the use of the VUV-IS to other electron attaching compounds (e.g. SF_6, HNO_3, etc.) that have small absorption cross sections in the VUV or have ionization potentials higher than 10.6 eV.

3.4 Q-CIMS Field Tests

Ground-based measurements of formic acid using the I^--CIMS with the VUV-IS were conducted at a rural site in Dongying, China, during the Ozone Photochemistry and Export from China Experiment (OPECE) campaign from March 20 to April 21, 2018. Continuous formic acid and j_{NO_2} measurements demonstrate reliable field operation of the lamp for long periods (Figure 7). A clogged mass flow controller on the inlet and a scroll pump failure caused brief measurement interruptions on March 27 and in early April. We could not obtain gas mixtures of CH_3I at this field location, so we used a liquid reservoir as CH_3I source. This led to using CH_3I levels of 100s of ppmv which may have accelerated degradation of the scroll pump tip seals. However, no direct problems were encountered with the VUV-IS and the lamp used in this work has been operational, with no obvious degradation of signal, for over 18 months.

3.5 TOF-CIMS Tests

The VUV-IS was found to give very similar signal levels to those obtained with a standard radioactive ion source (with an activity of ~16 mCi of ^{210}Po) on a TOF-CIMS. Both sources gave total reagent ion signals of ~10 MHz and similar sensitivity to both formic acid and Cl_2 of about 20-25 Hz/ppt. The I^- signal for both sources was ~6 MHz and $I^-(H_2O)$ signal was ~3 MHz. In addition, as illustrated in Figure 6, both sources gave very similar mass spectra for ambient air. The largest difference between the mass spectra were that the VUV-IS gave higher levels of I_3^- while the radioactive source gave higher levels of peaks corresponding to nitric acid (i.e. $I^-(HNO_3)$ and NO_3^-). Sensitivities as a function of CH_3I mixing ratio in the flow tube were also tested (Figure S2). Sensitivities to formic acid and Cl_2 increase with the CH_3I mixing ratio up to ~100 ppmv. The

https://doi.org/10.5194/amt-2020-13
Preprint. Discussion started: 3 February 2020


Atmospheric Measurement Techniques Discussions

sensitivities normalized to the reagent ion $I^-(H_2O)$ do not change with CH_3I mixing ratio and are the same obtained with the radioactive source. These results demonstrate that a VUV-IS can be used on a TOF-CIMS to obtain the same sensitivity, selectivity, and ion distribution as with a radioactive ion source.

4 Discussion

Clearly, the VUV-IS can generate I^- ions and mass spectra that are very similar to a radioactive ion source on both a TOF-CIMS and a Q-CIMS. For this reason, we think that the VUV-IS can replace radioactive ion sources in most I^--CIMS applications without any loss of measurement performance. Perhaps, the largest benefit of the VUV-IS is that it will expand the use of I^--CIMS to locations or situations where radioactivity is not allowed. The VUV-IS is also likely to be useful for laboratory flow tube or chamber studies that use CIMS as a detector (D'Ambro et al., 2017;Huang et al., 2017;Faxon et al., 2018). We have not found any interferences or issues that would limit application of a VUV-IS, though its application to measurement of individual species must be confirmed by further testing.

Using the VUV-IS requires attention to the possibility of interferences caused by the generation of photoelectrons from surfaces that can be attached by oxygen or other compounds in the sampled gas matrix. We were able to minimize this effect by using a flow geometry that shielded the flow tube from the VUV photons albeit at the expense of more than a factor of four in signal on the Q-CIMS. Similarly, the implementation of the VUV-IS on the TOF-CIMS successfully limited O_2^- production by passing the ion source flow through a small diameter tube that discriminated against light reaching the IMR. This issue might also be addressed by further improvements in geometry, the use of optical focusing elements, or higher levels of an absorber molecule.

The VUV-IS source requires an absorbing species to serve as a source of photoelectrons. Extending the use of the VUV-IS to other reagent ions such as SF_6^- (Nah et al., 2018), Br^- (Sanchez et al., 2016), NO_3^- (Eisele and Tanner, 1993), CF_3O^- (Crounse et al., 2006), and $CH_3CO_2^-$ (Veres et al., 2008) will most likely require the addition of an absorber such as C_6H_6. Although the use of CH_3I to produce I^- with the VUV-IS does not require an additional absorber, this application requires relatively high levels of CH_3I to obtain maximum sensitivities. Since CH_3I is a hazardous gas, higher levels of CH_3I could be problematic for some situations such as deployment in a highly regulated environment such as an aircraft. Higher levels of CH_3I may also necessitate protection of scroll pumps with scrubbers and traps. For these reasons, it may be preferable to use a low activity (Lee et al., 2019) or standard radioactive ion source for some applications.

One potential advantage of the VUV-IS is demonstrated by the lower background signals at masses corresponding to nitric acid (HNO_3). This is probably due to lower rates of nitrogen radical generation in the VUV-IS as the generated photons are much lower in energy (~10 eV) relative to the alpha particles (~5.4 MeV) from a ^{210}Po radioactive source. Additionally, the

https://doi.org/10.5194/amt-2020-13
Preprint. Discussion started: 3 February 2020


Atmospheric Measurement Techniques Discussions

VUV-IS does not produce ions when power is removed but radioactive decay is continuous. Consequently, interfering species can be continuously generated in a radioactive source, leading to build up of condensable species such as nitric acid. For these reasons, the VUV-IS may generate significantly lower levels of interferences than a radioactive source.

5 Conclusions

The VUV-IS described in this work can provide sensitivities and limits of detections that are at least comparable to those obtained with a radioactive ion source for both Q-CIMS and TOF-CIMS using I^- as a reagent ion. The VUV-IS is also reliable and can be safely deployed in remote field missions. These results demonstrate that the VUV-IS can eliminate the need for radioactivity with an I^--CIMS for most applications. The use of low IP absorbers, such as benzene, to generate photoelectrons in conjunction with high IP electron attaching compounds should also allow the generation of other reagent ions such as SF_6^-, CF_3O^-, NO_3^-. In summary, the VUV-IS has the potential to eliminate most of the use of radioactivity with CIMS instruments.

Data Availability

All of the data used in this manuscript is available upon request of the corresponding author.

Author Contributions

Yi Ji performed all of the Q-CIMS experiments and wrote the manuscript with assistance from Greg Huey. David Tanner assisted with all the experiments. Xinming Wang organized the OPECE campaign and provided the j_{NO_2} data. All of the authors were involved in data interpretation and commented on the manuscript. The TOF-CIMS experiments were performed by Patrick Veres, Andy Neuman, and Greg Huey.

Competing Interests

The authors declare that they have no conflicts of interest.

Acknowledgements

This work was also supported by NSF grant 1853930 and by NASA grant NNX15AT90G. The OPECE field mission was supported by NSF grant 1743401. This work was also supported in part by an EPA STAR grant R835882 awarded to the Georgia Institute of Technology. It has not been formally reviewed by the EPA. The views expressed in this document are solely those of the authors and do not necessarily reflect those of the EPA. EPA does not endorse any products or commercial services mentioned in this publication and EPA Grant. We thank Jianhui Tang for providing the RH data on the field. We also

https://doi.org/10.5194/amt-2020-13
Preprint. Discussion started: 3 February 2020

thank the Yellow River Delta Ecological Research Station of Coastal Wetland, which belongs to Yantai Institute of Coastal Zone Research, Chinese Academy of Sciences, for logistical support for the OPECE campaign.

References

Bertram, T. H., Kimmel, J. R., Crisp, T. A., Ryder, O. S., Yatavelli, R. L. N., Thornton, J. A., Cubison, M. J., Gonin, M., and Worsnop, D. R.: A field-deployable, chemical ionization time-of-flight mass spectrometer, Atmospheric Measurement Techniques, 4, 1471-1479, 10.5194/amt-4-1471-2011, 2011.

Capalbo, F. J., Benilan, Y., Fray, N., Schwell, M., Champion, N., Es-Sebbar, E. T., Koskinen, T. T., Lehocki, I., and Yelle, R. V.: New benzene absorption cross sections in the VUV, relevance for Titan's upper atmosphere, Icarus, 265, 95-109, 10.1016/j.icarus.2015.10.006, 2016.

Crounse, J. D., McKinney, K. A., Kwan, A. J., and Wennberg, P. O.: Measurement of gas-phase hydroperoxides by chemical ionization mass spectrometry, Analytical Chemistry, 78, 6726-6732, 10.1021/ac0604235, 2006.

D'Ambro, E. L., Lee, B. H., Liu, J. M., Shilling, J. E., Gaston, C. J., Lopez-Hilfiker, F. D., Schobesberger, S., Zaveri, R. A., Mohr, C., Lutz, A., Zhang, Z. F., Gold, A., Surratt, J. D., Rivera-Rios, J. C., Keutsch, F. N., and Thornton, J. A.: Molecular composition and volatility of isoprene photochemical oxidation secondary organic aerosol under low- and high-NOx conditions, Atmospheric Chemistry and Physics, 17, 159-174, 10.5194/acp-17-159-2017, 2017.

Eger, P. G., Helleis, F., Schuster, G., Phillips, G. J., Lelieveld, J., and Crowley, J. N.: Chemical ionization quadrupole mass spectrometer with an electrical discharge ion source for atmospheric trace gas measurement, Atmospheric Measurement Techniques, 12, 1935-1954, 10.5194/amt-12-1935-2019, 2019.

Eisele, F. L., and Tanner, D. J.: Measurement of the Gas-Phase Concentration of H2so4 and Methane Sulfonic-Acid and Estimates of H2so4 Production and Loss in the Atmosphere, Journal of Geophysical Research-Atmospheres, 98, 9001-9010, Doi 10.1029/93jd00031, 1993.

Faxon, C., Hammes, J., Le Breton, M., Pathak, R. K., and Hallquist, M.: Characterization of organic nitrate constituents of secondary organic aerosol (SOA) from nitrate-radical-initiated oxidation of limonene using high-resolution chemical ionization mass spectrometry, Atmos. Chem. Phys., 18, 5467-5481, 10.5194/acp-18-5467-2018, 2018.

Holmes, J. L., and Lossing, F. P.: Ionization Energies of Homologous Organic-Compounds and Correlation with Molecular-Size, Organic Mass Spectrometry, 26, 537-541, DOI 10.1002/oms.1210260603, 1991.

Huang, Y., Coggon, M., Zhao, R., Lignell, H., Bauer, M., Flagan, R., and Seinfeld, J.: The Caltech Photooxidation Flow Tube reactor: design, fluid dynamics and characterization, Journal Name: Atmospheric Measurement Techniques; Journal Volume: 10; Journal Issue: 3; Conference: null; Patent File Date: null; Patent Priority Date: null; Other Information: null; Related Information: null, Medium: X; Size: 839 to 867; Quantity: null; OS: null; Compatibility: null; Other: null, 2017.

Huey, L. G.: Measurement of trace atmospheric species by chemical ionization mass spectrometry: Speciation of reactive nitrogen and future directions, Mass Spectrometry Reviews, 26, 166-184, 10.1002/mas.20118, 2007.

Jost, C., Sprung, D., Kenntner, T., and Reiner, T.: Atmospheric pressure chemical ionization mass spectrometry for the detection of tropospheric trace gases: the influence of clustering on sensitivity and precision, International Journal of Mass Spectrometry, 223, 771-782, Pii S1387-3806(02)00963-6

Doi 10.1016/S1387-3806(02)00963-6, 2003.

Kauppila, T. J., Syage, J. A., and Benter, T.: Recent Developments in Atmospheric Pressure Photoionization-Mass Spectrometry, Mass Spectrometry Reviews, 36, 423-449, 2017.

Kurten, A., Rondo, L., Ehrhart, S., and Curtius, J.: Performance of a corona ion source for measurement of sulfuric acid by chemical ionization mass spectrometry, Atmospheric Measurement Techniques, 4, 437-443, 10.5194/amt-4-437-2011, 2011.

Lee, B. H., Lopez-Hilfiker, F. D., Mohr, C., Kurten, T., Worsnop, D. R., and Thornton, J. A.: An Iodide-Adduct High-Resolution Time-of-Flight Chemical-Ionization Mass Spectrometer: Application to Atmospheric Inorganic and Organic Compounds, Environmental Science & Technology, 48, 6309-6317, 10.1021/es500362a, 2014.

Lee, Y. R., Ji, Y., Tanner, D. J., and Huey, L. G.: A low activity ion source for measurement of atmospheric gases by CIMS, Atmos. Meas. Tech. Discuss., 2019, 1-15, 10.5194/amt-2019-452, 2019.

Liao, J., Sihler, H., Huey, L. G., Neuman, J. A., Tanner, D. J., Friess, U., Platt, U., Flocke, F. M., Orlando, J. J., Shepson, P. B., Beine, H. J., Weinheimer, A. J., Sjostedt, S. J., Nowak, J. B., Knapp, D. J., Staebler, R. M., Zheng, W., Sander, R., Hall, S. R., and Ullmann, K.: A comparison of Arctic BrO measurements by chemical ionization mass spectrometry and long path-differential optical absorption spectroscopy, Journal of Geophysical Research-Atmospheres, 116, Artn D00r02

10.1029/2010jd014788, 2011.

Liao, J., Huey, L. G., Liu, Z., Tanner, D. J., Cantrell, C. A., Orlando, J. J., Flocke, F. M., Shepson, P. B., Weinheimer, A. J., Hall, S. R., Ullmann, K., Beine, H. J., Wang, Y. H., Ingall, E. D., Stephens, C. R., Hornbrook, R. S., Apel, E. C., Riemer, D., Fried, A., Mauldin, R. L., Smith, J. N., Staebler, R. M., Neuman, J. A., and Nowak, J. B.: High levels of molecular chlorine in the Arctic atmosphere, Nature Geoscience, 7, 91-94, 10.1038/Ngeo2046, 2014.

Liu, X., Qu, H., Huey, L. G., Wang, Y., Sjostedt, S., Zeng, L., Lu, K., Wu, Y., Hu, M., Shao, M., Zhu, T., and Zhang, Y.: High Levels of Daytime Molecular Chlorine and Nitryl Chloride at a Rural Site on the North China Plain, Environmental Science & Technology, 51, 9588-9595, 10.1021/acs.est.7b03039, 2017.

Mohler, O., and Arnold, F.: Flow Reactor and Triple Quadrupole Mass-Spectrometer Investigations of Negative-Ion Reactions Involving Nitric-Acid - Implications for Atmospheric Hno3 Detection by Chemical Ionization Mass-Spectrometry, Journal of Atmospheric Chemistry, 13, 33-61, Doi 10.1007/Bf00048099, 1991.

Nah, T., Ji, Y., Tanner, D. J., Guo, H., Sullivan, A. P., Ng, N. L., Weber, R. J., and Huey, L. G.: Real-time measurements of gas-phase organic acids using SF6− chemical ionization mass spectrometry, Atmos. Meas. Tech., 11, 5087-5104, 10.5194/amt-11-5087-2018, 2018.

Nemeth, G. I., Selzle, H. L., and Schlag, E. W.: Magnetic Zeke Experiments with Mass Analysis, Chemical Physics Letters, 215, 151-155, Doi 10.1016/0009-2614(93)89279-Q, 1993.

Neuman, J. A., Trainer, M., Brown, S. S., Min, K. E., Nowak, J. B., Parrish, D. D., Peischl, J., Pollack, I. B., Roberts, J. M., Ryerson, T. B., and Veres, P. R.: HONO emission and production determined from airborne measurements over the Southeast US, Journal of Geophysical Research-Atmospheres, 121, 9237-9250, 10.1002/2016jd025197, 2016.

Olney, T. N., Cooper, G., and Brion, C. E.: Quantitative studies of the photoabsorption (4.5-488 eV) and photoionization (9-59.5 eV) of methyl iodide using dipole electron impact techniques, Chemical Physics, 232, 211-237, Doi 10.1016/S0301-0104(97)00368-6, 1998.

Osthoff, H. D., Roberts, J. M., Ravishankara, A. R., Williams, E. J., Lerner, B. M., Sommariva, R., Bates, T. S., Coffman, D., Quinn, P. K., Dibb, J. E., Stark, H., Burkholder, J. B., Talukdar, R. K., Meagher, J., Fehsenfeld, F. C., and Brown, S. S.: High levels of nitryl chloride in the polluted subtropical marine boundary layer, Nature Geoscience, 1, 324-328, 10.1038/ngeo177, 2008.

Phillips, G. J., Pouvesle, N., Thieser, J., Schuster, G., Axinte, R., Fischer, H., Williams, J., Lelieveld, J., and Crowley, J. N.: Peroxyacetyl nitrate (PAN) and peroxyacetic acid (PAA) measurements by iodide chemical ionisation mass spectrometry: first analysis of results in the boreal forest and implications for the measurement of PAN fluxes, Atmospheric Chemistry and Physics, 13, 1129-1139, 10.5194/acp-13-1129-2013, 2013.

Priestley, M., le Breton, M., Bannan, T. J., Worrall, S. D., Bacak, A., Smedley, A. R. D., Reyes-Villegas, E., Mehra, A., Allan, J., Webb, A. R., Shallcross, D. E., Coe, H., and Percival, C. J.: Observations of organic and inorganic chlorinated

https://doi.org/10.5194/amt-2020-13
Preprint. Discussion started: 3 February 2020

compounds and their contribution to chlorine radical concentrations in an urban environment in northern Europe during the wintertime, Atmospheric Chemistry and Physics, 18, 13481-13493, 10.5194/acp-18-13481-2018, 2018.

Sanchez, J., Tanner, D. J., Chen, D., Huey, L. G., and Ng, N. L.: A new technique for the direct detection of HO2 radicals using bromide chemical ionization mass spectrometry (Br-CIMS): initial characterization, Atmos. Meas. Tech., 9, 3851-3861, 10.5194/amt-9-3851-2016, 2016.

Skalny, J. D., Horvath, G., and Mason, N. L.: Mass spectrometric analysis of small negative ions (e/m < 100) produced by Trichel pulse negative corona discharge fed by ozonised air, Journal of Optoelectronics and Advanced Materials, 9, 887-893, 2007.

Slusher, D. L., Huey, L. G., Tanner, D. J., Flocke, F. M., and Roberts, J. M.: A thermal dissociation--chemical ionization mass spectrometry(TD-CIMS) technique for the simultaneous measurement of peroxyacyl nitrates and dinitrogen pentoxide, Journal of Geophysical Research: Atmospheres, 109, 10.1029/2004JD004670, 2004.

Thornton, J. A., Kercher, J. P., Riedel, T. P., Wagner, N. L., Cozic, J., Holloway, J. S., Dube, W. P., Wolfe, G. M., Quinn, P. K., Middlebrook, A. M., Alexander, B., and Brown, S. S.: A large atomic chlorine source inferred from mid-continental reactive nitrogen chemistry, Nature, 464, 271-274, 10.1038/nature08905, 2010.

Veres, P., Roberts, J. M., Warneke, C., Welsh-Bon, D., Zahniser, M., Herndon, S., Fall, R., and de Gouw, J.: Development of negative-ion proton-transfer chemical-ionization mass spectrometry (NI-PT-CIMS) for the measurement of gas-phase organic acids in the atmosphere, International Journal of Mass Spectrometry, 274, 48-55, 10.1016/j.ijms.2008.04.032, 2008.

Veres, P., Gilman, J. B., Roberts, J. M., Kuster, W. C., Warneke, C., Burling, I. R., and de Gouw, J.: Development and validation of a portable gas phase standard generation and calibration system for volatile organic compounds, Atmos. Meas. Tech., 3, 683-691, 10.5194/amt-3-683-2010, 2010.

Wang, X. F., Wang, T., Xue, L. K., Nie, W., Xu, Z., Poon, S. C. N., and Wang, W. X.: Peroxyacetyl nitrate measurements by thermal dissociation-chemical ionization mass spectrometry in an urban environment: performance and characterizations, Frontiers of Environmental Science & Engineering, 11, ARTN 3

10.1007/s11783-017-0925-7, 2017.

https://doi.org/10.5194/amt-2020-13
Preprint. Discussion started: 3 February 2020

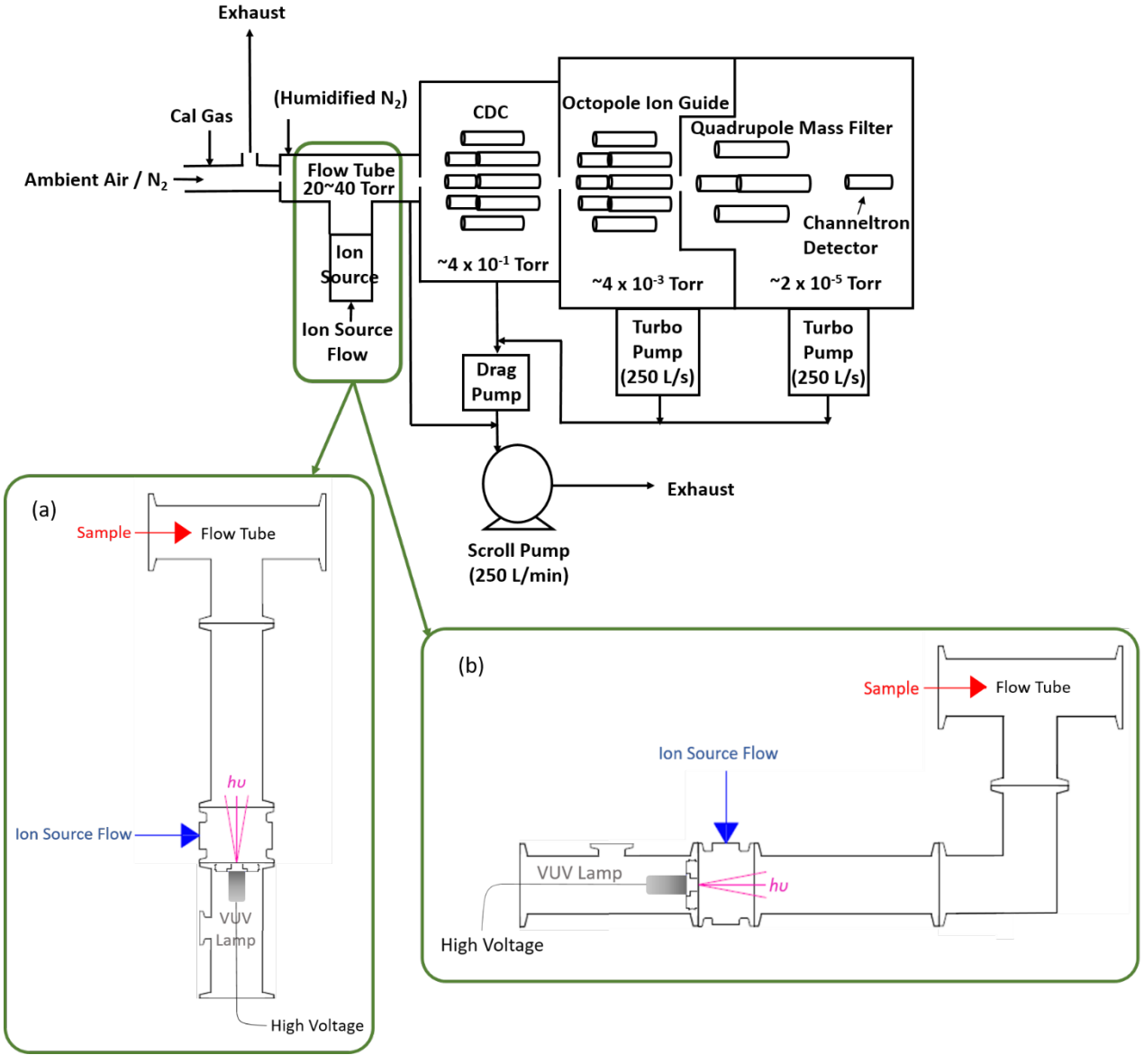

Figure 1: Diagram of the I^--Q-CIMS system with a VUV-IS in two different configurations. Configuration (a) provides the most direct route for the generated ions but also directly illuminates the flow tube. Configuration (b) shields the flow tube from the VUV photons by inserting a QF 40 elbow between the photoionization region and the flow tube.

https://doi.org/10.5194/amt-2020-13
Preprint. Discussion started: 3 February 2020

Atmospheric Measurement Techniques Discussions

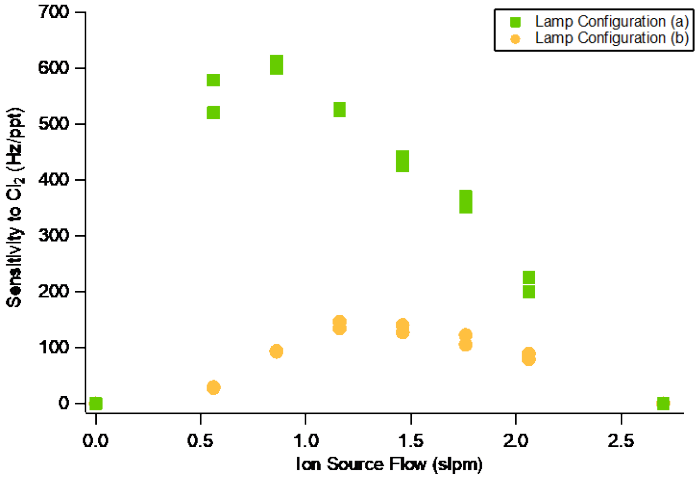

Figure 2: Q-CIMS sensitivity to $Cl_2 \cdot I^-$ (m/z = 197 amu) as a function of total ion source flow using the VUV-IS with lamp configuration (a) and (b).

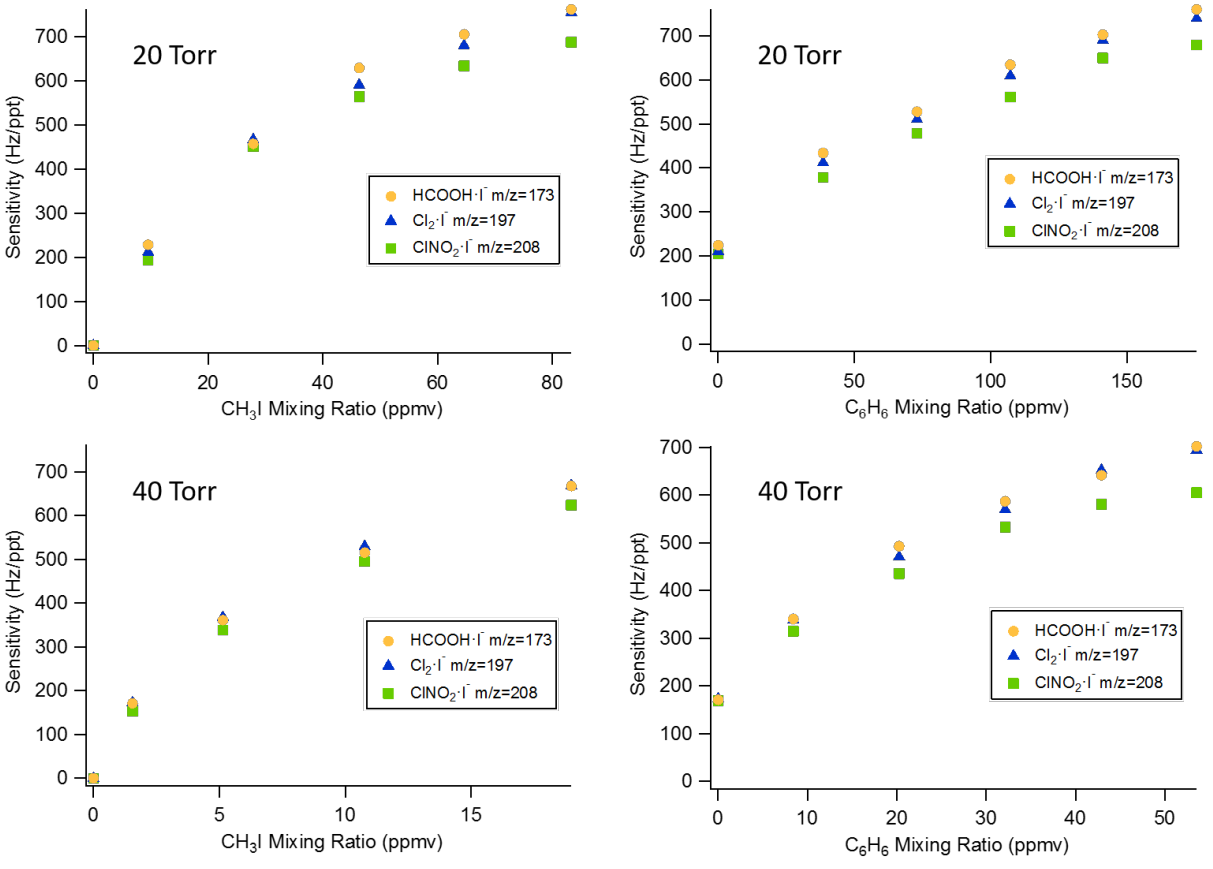

Figure 3: Q-CIMS using VUV-IS configuration (a): Upper left panel - sensitivity as a function of CH_3I at 20 Torr. Upper right panel- sensitivity as a function of C_6H_6 at 20 Torr. Lower left panel- sensitivity as a function of. CH_3I at 40 Torr. Lower right panel - sensitivity as a function of C_6H_6 at 40 Torr.

https://doi.org/10.5194/amt-2020-13
Preprint. Discussion started: 3 February 2020

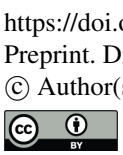

Atmospheric Measurement Techniques Discussions

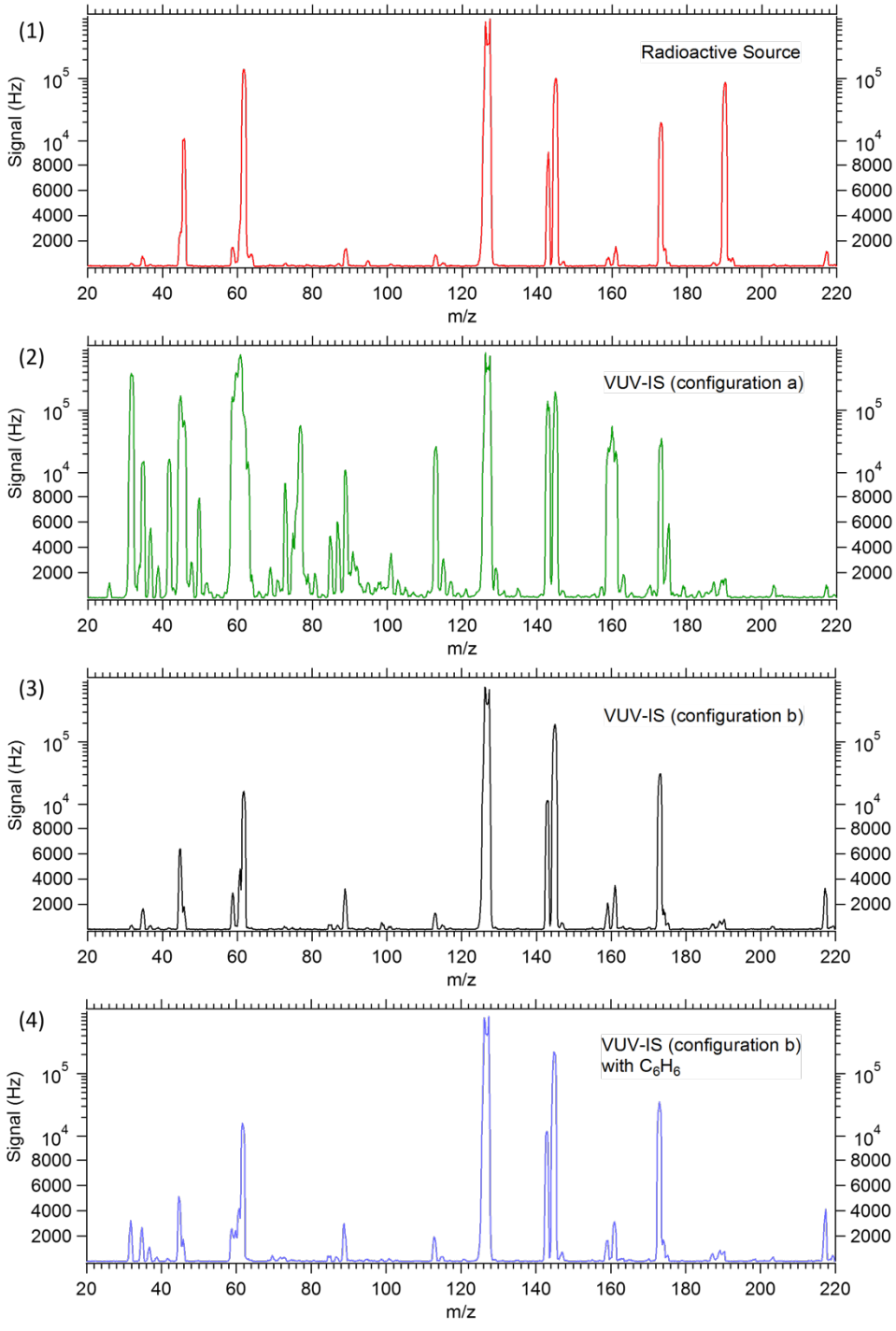

Figure 4: Mass spectra of ambient air from a Q-CIMS with (1) a standard radioactive ion source, (2) VUV-IS in configuration (a), (3) VUV-IS in configuration (b), and (4) VUV-IS in configuration (b) with ~100 ppmv of C_6H_6 and ~10 ppmv of CH_3I. Note that the I^- signal is saturated in all mass spectra.

https://doi.org/10.5194/amt-2020-13
Preprint. Discussion started: 3 February 2020

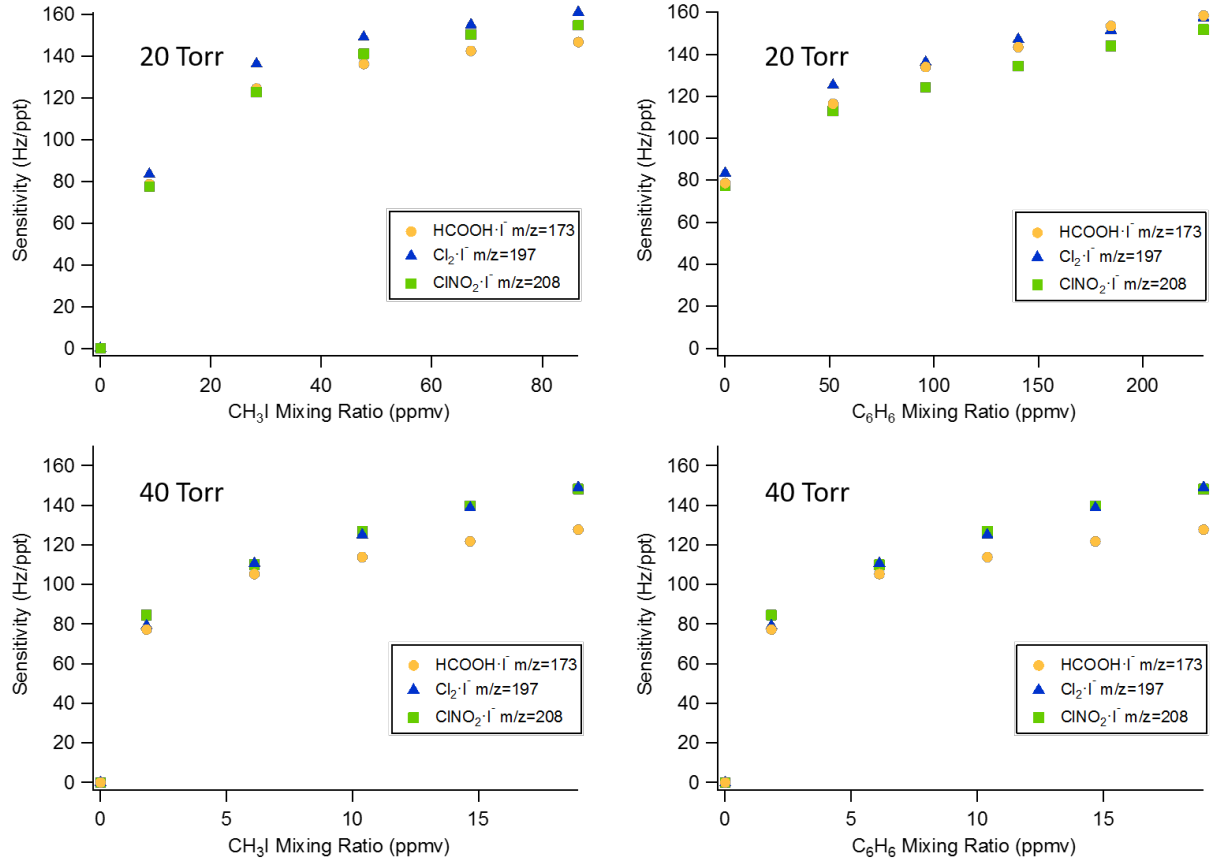

400

Figure 5: Q-CIMS using VUV-IS configuration (b): Upper left panel - sensitivity as a function of CH_3I at 20 Torr. Upper right panel- sensitivity as a function of C_6H_6 at 20 Torr. Lower left panel- sensitivity as a function of. CH_3I at 40 Torr. Lower right panel - sensitivity as a function of C_6H_6 at 40 Torr.

https://doi.org/10.5194/amt-2020-13
Preprint. Discussion started: 3 February 2020

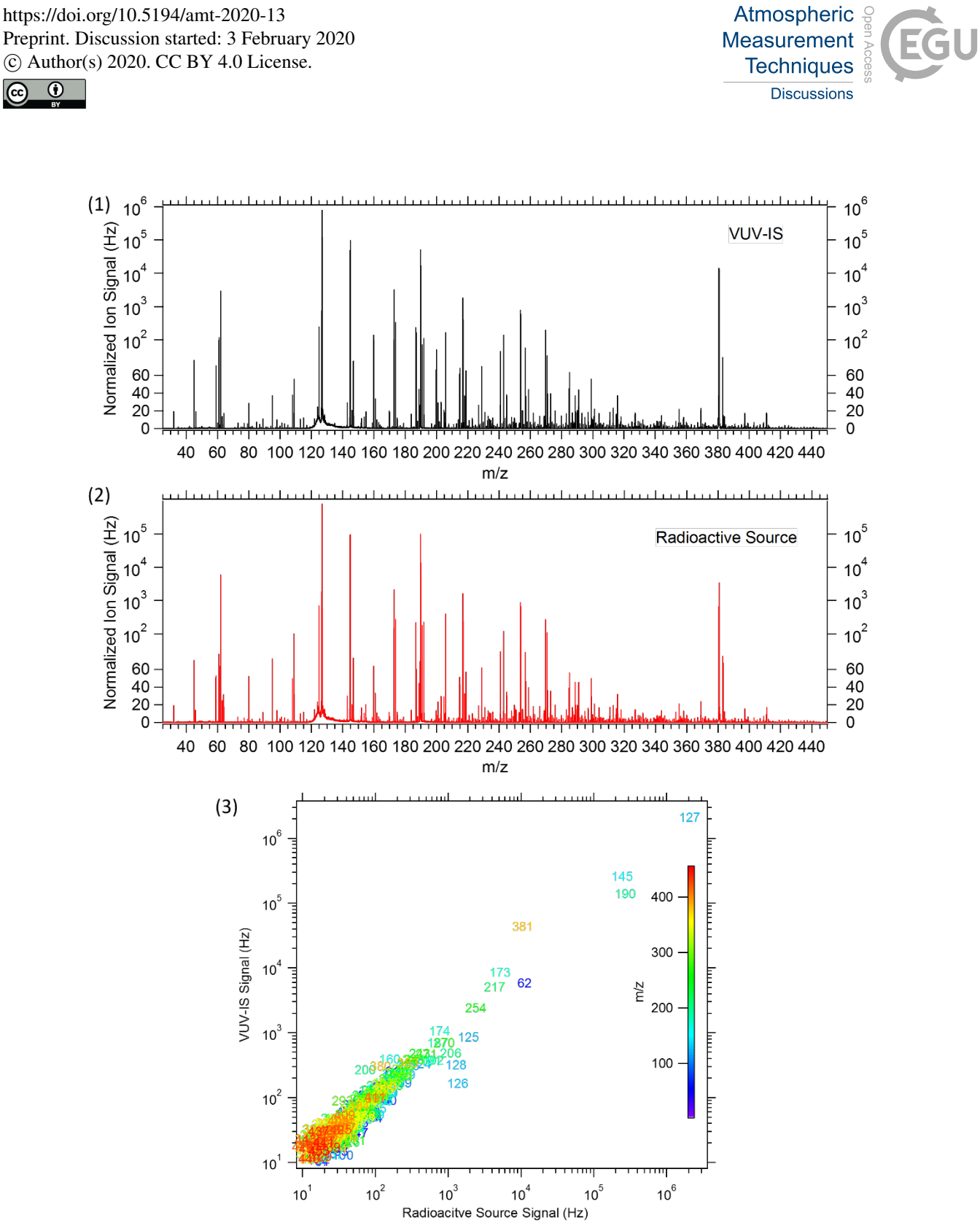

405

Figure 6. Mass spectra of ambient air in Boulder, CO from a TOF-CIMS with (1) a VUV-IS (2) a radioactive source. The bottom panel (3) is a correlation plot of the individual mass signals with the VUV-IS versus those obtained with a radioactive source, with each ion labeled by its nominal mass.

https://doi.org/10.5194/amt-2020-13
Preprint. Discussion started: 3 February 2020

Atmospheric Measurement Techniques Discussions

410

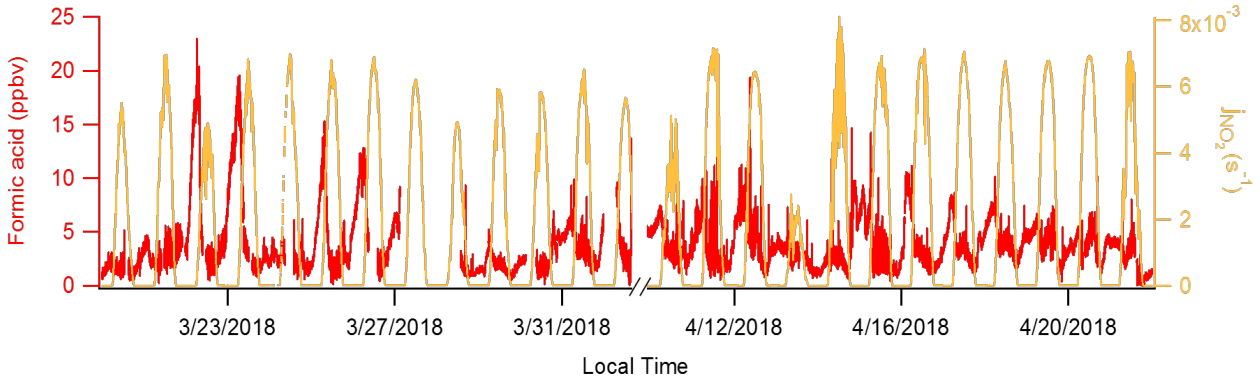

Figure 7: Time series of formic acid concentration and j_{NO_2} during the OPECE field campaign.

https://doi.org/10.5194/amt-2020-13
Preprint. Discussion started: 3 February 2020

Atmospheric Measurement Techniques Discussions

Table 1: Experiment conditions, sensitivities and limits of detection (LODs) for VUV-IS configuration (b)

Exp.		CH_3I only	CH_3I and C_6H_6	CH_3I only	CH_3I and C_6H_6
flow tube pressure (Torr)		20	20	40	40
CH_3I mixing ratio (ppmv)		8.8 – 86.5	8.8	1.8 – 19.0	1.8
C_6H_6 mixing ratio (ppmv)		0	0 – 229.2	0	0 – 58.9
formic acid	sensitivity (Hz $pptv^{-1}$) [a]	79 - 147	79 - 158	77 - 128	77 - 157
	1 min LOD (pptv) [a, b]	0.78 – 0.74	0.78 – 0.67	0.88 – 0.62	0.88 – 0.67
Cl_2	sensitivity (Hz $pptv^{-1}$) [a]	83 – 161	83 - 157	79 - 149	79 - 166
	1 min LOD (pptv) [a, b]	0.82 – 0.72	0.82 – 0.68	0.92 – 0.64	0.92 – 0.52
$ClNO_2$	sensitivity (Hz $pptv^{-1}$) [a]	77 - 154	77 - 152	85 - 148	85 - 138
	1 min LOD (pptv) [a, b]	0.45 – 0.24	0.45 – 0.31	0.43 – 0.17	0.43 – 0.19

[a] Sensitivities and detection limits are for $HCOOH{\cdot}I^-$ (m/z = 173 amu), $Cl_2{\cdot}I^-$ (m/z = 197 amu) and $ClNO_2{\cdot}I^-$ (m/z = 208 amu).

[b] Signal to noise ratio = 3:1

Table 2: Experiment conditions, sensitivities and limits of detection (LODs) for VUV-IS configuration (a)

Exp.		CH_3I only	CH_3I and C_6H_6	CH_3I only	CH_3I and C_6H_6
flow tube pressure (Torr)		20	20	40	40
CH_3I mixing ratio (ppmv)		9.6 - 83	9.6	1.6 – 19	1.6
C_6H_6 mixing ratio (ppmv)		0	0 - 175	0	0 - 54
formic acid	sensitivity (Hz $pptv^{-1}$) [a]	228 - 761	225 - 761	171 - 591	171 - 703
	1 min LOD (pptv) [a, b]	0.44 – 0.36	0.59 – 0.23	0.52 – 0.28	0.68 – 0.21
Cl_2	sensitivity (Hz $pptv^{-1}$) [a]	212 – 754	210 - 740	173 - 605	173 - 694
	1 min LOD (pptv) [a, b]	0.56 – 0.30	0.49 – 0.27	0.62 – 0.24	0.48 – 0.24
$ClNO_2$	sensitivity (Hz $pptv^{-1}$) [a]	193 - 687	204 - 679	153 - 570	169 - 605
	1 min LOD (pptv) [a, b]	0.22 – 0.12	0.20 – 0.10	0.07 – 0.05	0.12 – 0.07

[a] Sensitivities and detection limits are for $HCOOH{\cdot}I^-$ (m/z = 173 amu), $Cl_2{\cdot}I^-$ (m/z = 197 amu) and $ClNO_2{\cdot}I^-$ (m/z = 208 amu).

[b] Signal to noise ratio = 3:1